An analysis of the effects of different network-based ionosphere estimation models on rover positioning accuracy

Dorota A. Grejner-Brzezinska[1], Pawel Wielgosz[1,2], Israel Kashani[1,3], Dru A. Smith[4], Paul S. J. Spencer[4], Douglas S. Robertson[4] and Gerald L. Mader[4]

[1] The Ohio State University, SPIN LAB, 470 Hitchcock Hall, 2070 Neil Ave., Columbus, OH 43210-1275
 e-mail: dbrzezinska@osu.edu; Tel: (614) 292-8787; Fax: (614) 292-2957

[2] University of Warmia and Mazury – UWM

[3] Israel Institute of Technology – Technion

[4] National Geodetic Survey – NGS

Abstract. The primary objective of this paper is to test several methods of modeling the ionospheric corrections derived from a reference GPS network, and to study the impact of the models' accuracy on the user positioning results. The five ionospheric models that are discussed here are: (1) network RTK (NR) carrier phase-based model — MPGPS-NR, (2) absolute, smoothed pseudorange-based model — MPGPS-P4, (3) IGS Global Ionosphere Model — GIM, (4) absolute model based on undifferenced dual-frequency ambiguous carrier phase data — ICON, and (5) carrier phase-based data assimilation method — MAGIC. Methods 1–4 assume that the ionosphere is an infinitesimal single layer, while method (5) considers the ionosphere as a 3D medium. The test data set was collected at the Ohio Continuously Operating Reference Stations (CORS) network on August 31, 2003. A 24-hour data set, representing moderate ionospheric conditions (maximum Kp = 2o), was processed. The ionospheric reference "truth" in double-difference (DD) form was generated from the dual-frequency carrier phase data for two selected baselines, ~60 and ~100 km long, where one station was considered as a user receiver at an unknown location (simulated rover). The five ionospheric models were used to generate the DD ionospheric corrections for the rover, and were compared to the reference "truth." The quality statistics were generated and discussed. Examples of instantaneous ambiguity resolution and RTK positioning are presented, together with the accuracy requirements for the ionospheric corrections, to assure integer ambiguity fixing.

1 Introduction

One of the major limiting factors in GPS-based precise positioning is the ionosphere-induced propagation delay that, if not properly accounted for, may result in significant positioning errors. This is particularly true for single frequency data, reducing the length of the effective baseline to 10–15 km. While dual-frequency carrier phase measurements can form an ionosphere-free linear combination that removes first-order ionospheric errors, the integer ambiguities can be fixed only for short baselines, since the ionospheric error decorrelates with distance. The ionospheric signal delay is a function of the total electron content (TEC). TEC is defined as the total number of electrons contained in a column with a cross-sectional area of 1 m^2 along the signal path. TEC displays primarily day-to-night variations, but also depends on the geomagnetic latitude, time of year, and the sunspot cycle. It is measured in electron/m^2, where one total electron content unit (TECU) is defined as 10^{16} electron/m^2. One meter of the ionospheric delay (or advance) on the first GPS frequency corresponds to 6.16 TECU, or one TECU causes 0.162 m delay.

The ability to remove the ionospheric delay from GPS data can increase the performance of the integer

ambiguity resolution (AR) process, and improve the computational efficiency of the search process. However, due to the high-level variability of TEC, empirical ionospheric models do not provide sufficient accuracy to support high-precision positioning applications. On the other hand, if external information on the integrated TEC between pairs of satellites and receivers is provided based on real observation data, the base-rover separation can be significantly extended, resulting in a virtually "distance-independent" precise positioning. The external ionospheric information provides an important constraint for accurate and rapid carrier phase AR. An alternative approach is to estimate the double-difference (DD) ionospheric delay parameters in the positioning adjustment model. However, the underlying mathematical model becomes weaker, and as a consequence the required observation sessions become longer (Odijk, 2000); thus, this method does not apply to rapid static or kinematic algorithms where the occupation time is of the order of seconds to minutes.

Several methods have been proposed to estimate and model the ionospheric corrections from the ground-based GPS data from the Continuously Operating Reference Stations (CORS) network, and the mathematical representation of the ionospheric electron density field have been studied (see, for example Odijk, 2000 and 2001; Schaer, 1999; Wielgosz *et al.*, 2003; Kashani *et al.*, 2004a; Smith, 2004; Spencer *et al.*, 2004) to support network-based real-time kinematic (RTK) (see, for example, Vollath *et al.*, 2000; Rizos, 2002; Wanninger, 2002; Grejner-Brzezinska *et al.*, 2004a and 2004b). The most challenging among these methods is the instantaneous AR approach (Kim and Langley, 2000), where for each individual observation epoch a new integer ambiguity solution is obtained using only the current epoch data (Bock *et al.*, 2003). Consequently, this method is resistant to negative effects of cycle slips and gaps, and can provide centimeter-level positioning accuracy immediately, without any delay needed for initialization (or re-initialization). However, to successfully resolve the ambiguities instantaneously over long distances, external atmospheric corrections of high accuracy are required (Odijk, 2001; Kashani *et al.*, 2004b).

This paper presents the accuracy analysis of several methods of ionospheric correction modeling in comparison to reference "truth," using the Multi Purpose GPS Processing Software (MPGPS™) developed at the Satellite Positioning and Inertial Navigation (SPIN) group at The Ohio State University. The ionospheric corrections are represented by the DD ionospheric delays estimated directly from dual-frequency carrier phase data constrained by the integer ambiguities. Examples of the positioning accuracy, supported by instantaneous AR, achieved as a function of the ionospheric correction

quality are also presented and discussed. The five ionospheric models tested are listed below.

MPGPS-NR — Network RTK (NR) carrier phase-based model, decomposed from DD ionospheric delays (Kashani *et al.*, 2004a),

MPGPS-P4 — Absolute, smoothed pseudorange-based method (Wielgosz *et al.*, 2003),

IGS GIM — International GPS Service (IGS) global ionospheric map (GIM). IGS GIM is a combination of several different ionosphere models provided by the IGS Ionosphere Associate Analysis Centers (Schaer, 1999),

ICON — Absolute model based on undifferenced dual-frequency ambiguous carrier phase data (Smith, 2004),

MAGIC — Pseudorange-leveled carrier phase-based data assimilation method (Spencer *et al.*, 2004).

Methods 1–4 assume that the ionosphere is an infinitesimal single layer, while method 5 considers the ionosphere as a 3D medium. In terms of spatial coverage, methods 1 and 2 are considered local; methods 4 and 5 are regional, while method 3 offers global coverage. MAGIC and ICON (4 and 5) are the two NGS ionosphere models derived for the continental United States. These two models use CORS GPS data, and provide the ionospheric corrections with a three-day delay. Both models are prototypes, a part of ongoing research projects, and are currently available to the general public for testing and evaluation purposes (http://www.noaanews.noaa.gov/stories2004/s2333.htm).

2 Approach and methodology

This section provides a brief description of the algorithms and methods applied to the aforementioned ionosphere estimation models. In addition, the AR and rover positioning algorithms are also briefly discussed. More details can be found in the references provided in each section.

2.1 The ionospheric models

2.1.1 The reference "truth" model — MPGPS-L4

The fundamental mathematical model for the network-based adjustment, using dual-frequency carrier phase and pseudorange data from the reference stations, is described by Eq. (1). The system of equations (1) written for the entire network is solved for each epoch of observations using a generalization-based sequential least-squares adjustment with stochastic constraints (Kashani *et al.*, 2004a).

$$\Phi_{1,ij}^{kl} - \rho_{ij}^{kl} - (\alpha_i^k T_i - \alpha_i^l T_i - \alpha_j^k T_j + \alpha_j^l T_j) + I_{ij}^{kl} \qquad - \lambda_1 N_{1,ij}^{kl} = 0$$

$$\Phi_{2,ij}^{kl} - \rho_{ij}^{kl} - (\alpha_i^k T_i - \alpha_i^l T_i - \alpha_j^k T_j + \alpha_j^l T_j) + (\upsilon_1^2 / \upsilon_2^2) I_{ij}^{kl} - \lambda_2 N_{2,ij}^{kl} = 0$$

$$P_{1,ij}^{kl} - \rho_{ij}^{kl} - (\alpha_i^k T_i - \alpha_i^l T_i - \alpha_j^k T_j + \alpha_j^l T_j) - I_{ij}^{kl} \qquad = 0$$

$$P_{2,ij}^{kl} - \rho_{ij}^{kl} - (\alpha_i^k T_i - \alpha_i^l T_i - \alpha_j^k T_j + \alpha_j^l T_j) - (\upsilon_1^2 / \upsilon_2^2) I_{ij}^{kl} \qquad = 0$$

(1)

where:

i, j receiver indices,

k, l satellite indices,

$\Phi_{n,ij}^{kl}$ DD phase observation on frequency n (n=1,2),

$P_{n,ij}^{kl}$ DD code observation on frequency n,

ρ_{ij}^{kl} DD geometric distance,

$T_{i,j}$ tropospheric total zenith delay (TZD),

α_i^k troposphere mapping function,

I_{ij}^{kl} DD ionospheric delay,

υ_1, υ_2 L1 and L2 frequencies,

λ_1, λ_2 GPS frequency wavelengths on L1 and L2,

$N_{1,ij}^{kl}, N_{2,ij}^{kl}$ DD carrier phase ambiguities on L1 and L2.

The unknown parameters are undifferenced total zenith delay (TZD), provided for individual stations ($T_{i,j}$), DD ionospheric delays (I_{ij}^{kl}), and DD ambiguities ($N_{1,ij}^{kl}, N_{2,ij}^{kl}$). The coordinates of the permanent stations (CORS) are considered known (obtained from a 24-hour solution using the BERNESE software (Hugentobler *et al.*, 2001)), which makes the AR for the reference network much easier to perform, even for long-range distances (i.e., ~200 km between the CORS stations). All the parameters are constrained to some a priori information, which may consist of empirical values (e.g., 30–50 cm for the DD ionospheric delays, depending on the baseline length, local time and satellite elevation angle), as well as variance-covariance matrix for the known CORS coordinates. The Least-squares AMBiguity Decorrelation Adjustment (LAMBDA) is used to fix the ambiguities to their integer values (Teunissen, 1994). The validation procedure used is the AR success rate (Teunissen *et al.*, 2002), which represents the probability of estimating the correct integers.

After the DD ambiguities associated with the reference receivers have been fixed to their correct integer values, the "true" DD ionospheric delay can be correctly

estimated using the geometry-free linear combination described by Eq. (2):

$$L_{ij,4}^{kl} + \xi_4 I_{ij}^{kl} - (\lambda_1 N_{1,ij}^{kl} - \lambda_2 N_{2,ij}^{kl}) = 0 \qquad (2)$$

where:

$$L_{ij,4}^{kl} = L_{ij,1}^{kl} - L_{ij,2}^{kl} \text{ and } \quad \xi_4 = 1 - \frac{\upsilon_1^2}{\upsilon_2^2} \approx -0.647$$

It can be seen from Eq. (2) that if the dual-frequency ambiguity parameters $N_{1,ij}^{kl}$ and $N_{2,ij}^{kl}$ are fixed to their integers, the only remaining unknown parameter, I_{ij}^{kl}, representing the DD ionospheric delay on L1, can be estimated with a few-millimeter accuracy, corresponding primarily to the noise on the DD carrier phase observables.

2.1.2 The carrier phase DD model — MPGPS-NR

The network-based approach presented is Section 2.1.1 was also used to derive the network-based ionospheric corrections (MPGPS-NR). In this model, the zero difference (ZD) ionospheric delays (i.e., one-way, biased) were obtained by decomposing the network-derived DD delays, and interpolated for the rover location (KNTN). This was done for all satellites/epochs used in the analyses presented in Section 3. The network solution did not include the selected rover observations. It should be mentioned that for an individual baseline and *n* DD delays the rigorous decomposition is not possible without the a priori knowledge of at least two ZD values; there are only *n-2* linearly independent DD observation equations, thus the system is undetermined. To regularize the normal matrix, independent constraints on at least two ZD delays are needed, or loose constraints can be introduced to the diagonal of the normal matrix. Both methods result in a biased estimate. Although the reconstruction of the DD delays from the interpolated ZD delays may still include some amount of residual biases, the resulting DD delays are generally of sufficient accuracy to enable fast AR with only a few epochs of data (see Kashani *et al.*, 2004a).

2.1.3 The smoothed pseudorange model — MPGPS-P4

In this approach (Wielgosz *et al*., 2003) dual-frequency GPS carrier phase data are used to smooth the pseudorange observations collected at the reference station network (Springer, 1999). After the smoothing procedure, the pseudoranges are effectively replaced by the carrier phase observations with approximated (real-value) ambiguities. The differential code biases (DCBs) for the satellites are provided by IGS (ftp://gage.upc.es/pub/gps_data/GPS_IONO), and for the receivers, are derived from the calibration performed with the BERNESE software (Hugentobler *et al*., 2001). The instantaneous absolute ionospheric delay I_i^k is computed from Eq. (3):

$$I_i^k = (\tilde{P}_{i,4}^k - c(\Delta b^k + \Delta b_i)) / \xi_4 \qquad (3)$$

where:

i, j, k, l indices are the same as in Section 2.1.1,

$\tilde{P}_{i,n}^k$ carrier-smoothed code observation on frequency n (n=1,2),

$\tilde{P}_{i,4}^k$ geometry-free linear combination of smoothed code observations $\tilde{P}_{i,4}^k = \tilde{P}_{i,1}^k - \tilde{P}_{i,2}^k$,

c speed of light,

$\Delta b^k, \Delta b_i$ DCB for satellite k, and receiver i, respectively,

ξ_4 coefficient converting ionospheric delay on P_4 to P_1 delay (Eq. (2)).

The ionospheric delay is the following function of TEC (Schaer, 1999):

$$I_i^k = \pm \frac{C_x}{2} TEC \upsilon_1^{-2} = \xi_{TEC} TEC \qquad (4)$$

where the proportionality factor $\dfrac{C_x}{2}$ = 40.3 $\times 10^{16}$ ms^{-2}/TECU, and the ionospheric delay caused by 1 TECU on $L1$ is ξ_{TEC} = 0.162 m/TECU.

2.1.4 The IGS GIM

The IGS GIMs are derived as a weighted combination of several different models developed independently by the IGS Ionosphere Associate Analysis Centers. The combined maps have a spatial resolution of 2.5º and 5.0º in latitude and longitude, respectively, and a 2-hour temporal resolution (Feltens and Jakowski, 2002). IGS

GIMs assume a single layer model with the layer height, H, at 450 km. To convert the vertical TEC (VTEC) from GIMs into the line-of-sight slant TEC, a modified single-layer model (MSLM) mapping function is adopted (Eq. 5).

$$F(Z) = \frac{1}{\cos(z')} \qquad (5)$$

with:

$$\sin(z') = \frac{R}{R + H} \sin(\alpha z)$$

$$TEC = VTEC / \cos(z')$$

where: $F(z)$ is the mapping function, R is the Earth's radius, z is the vertical angle to the satellite, z' is the angle between the topocentric direction to the satellite and the normal to the ionospheric layer through the pierce point (piercing angle), and α is a scaling factor. GIMs provide absolute TEC in the IONEX format (Schaer *et al*., 1998). In this study, the ionospheric delays were interpolated for the rover and base receiver locations using kriging; they can subsequently be used to form DD corrections in the rover-positioning step.

2.1.5 The carrier phase absolute model — ICON

This method of computing absolute (unambiguous) levels of TEC (and subsequently L1 and L2 delays) from a ground-based network of GPS receivers requires dual-frequency carrier phase data. The ionosphere is assumed to lie in a single layer of constant ellipsoidal height of 300 km, and the geographic locations of the GPS ground stations must allow simultaneous observation of satellites by a number of stations. Slant TEC derived from GPS measurements is converted to VTEC, as shown in Eq. (5). Considering dual-frequency data, one can derive Eq. (6) to estimate the TEC difference between consecutive epochs m and n, where κ corresponds to $C_x / 2$ in Eq. (4). Using Eq. (5), the TEC difference can be further converted to the difference in VTEC, as shown in Eq. (7), which represents the ambiguous VTEC as a function of the unknown absolute TEC at epoch m. In these formulas, φ_1 and φ_2 are the carrier phase data in cycles.

$$\Delta TEC^{m,n} = TEC^m - TEC^n =$$

$$\left(\frac{1}{\kappa}\right)\left(\frac{1}{\upsilon_1^2} - \frac{1}{\upsilon_2^2}\right)^{-1}\left(\Delta\varphi_1^{m,n} - \Delta\varphi_2^{m,n}\right) \qquad (6)$$

$$\Delta VTEC^{m,n} = VTEC^n - VTEC^m =$$

$$TEC^n \cos(z'^n) - TEC^m \cos(z'^m) = \qquad (7)$$

$$\Delta TEC^{m,n} \cos(z'^n) + TEC^m(\cos(z'^n) - \cos(z'^m))$$

In order to estimate the bias (as only TEC time-difference can be obtained from (6) or (7)), a concept of track crossover is introduced, which is the fundamental notion of this method. The term crossover is related here to any two satellite tracks formed by the ionosphere pierce points, that fall within some acceptably small tolerance (in both space and time) of one another. Considering three tracks forming a triangle, as shown in Figure 1, each of the three tracks has one unknown bias (b_1, b_2 and b_3), corresponding to the absolute TEC value at some initial epoch. If these biases were known, the absolute values of TEC and VTEC at every epoch can be computed using the biases and ΔVTEC defined in Eq. (7). Each crossover A, B and C in Figure 1 forms a unique constraint for the system (Eq. 8), which allows for absolute estimation of VTEC. Adjoining "triangles," shown in Figure 1, provide more constraints introducing redundancy to the system. For more details on this method, see (Smith, 2004). In this study, the ionospheric delay values were computed for entire continental U.S., using around 340 stations; normally, for stations not included in the computations, TEC (and delays) can be interpolated for the station/satellite pair.

$$VTEC_1^A = VTEC_3^A = VTEC^A$$

$$VTEC_1^B = VTEC_2^B = VTEC^B \qquad (8)$$

$$VTEC_2^C = VTEC_3^C = VTEC^C$$

2.1.6 The carrier phase tomographic model — MAGIC

A method used here to reconstruct the 3D Earth ionospheric electron density field using a land-based network of GPS receivers is referred to as the data assimilation method. It uses a Kalman filter and can combine data from various sources to obtain inversions in three dimensions (Spencer *et al.*, 2004). The primary problem of the data assimilation method, which requires some form of mathematical regularization, transpires from the fact that the method is essentially a very poorly constrained linear least squares problem. Continuity relationships, defining the smoothness or entropy of the solution, are often used regularization techniques in tomographic methods (2D and 3D), while in cases of data assimilation methods, an a priori model estimate of the solution along with an estimate of its covariance are used. MAGIC uses an optional mapping function to alter the representation of the Kalman filter state vector in terms of a set of discrete radial empirical orthonormal functions (EOFs) to enable a more concise representation of the state vector (the ionospheric electron density field) in three dimensions (Spencer *et al.*, 2004). The EOFs were formed by applying singular value decomposition to a set

of model profiles generated by IRI95 (International Reference Ionosphere; see, for example, Bilitza, 1997). The dominant term, EOF_1, represents a mean ionospheric profile. Examples of empirical orthonormal functions are illustrated in Figure 2.

The carrier phase geometry-free linear combination (L4) leveled to the pseudorange is used as the GPS observable. The solutions are quantized with 15-minute time-steps. In this study, about 150 CORS and IGS stations were used for the TEC (converted to ionospheric delay) estimation for the continental US. For more details on this method, see (Spencer *et al.*, 2004).

2.2 The kinematic positioning algorithm

The concept of long-range instantaneous RTK GPS presented here is based on the atmospheric corrections derived from the GPS observations collected by the reference network that supports the rover positioning. The data reduction algorithm operates in the DD mode, which requires receiving observations from at least one reference station, together with the atmospheric corrections, i.e., tropospheric, T_{ij}^{kl}, and ionospheric, I_{ij}^{kl}, as shown in Eq. 9.

$$
\begin{aligned}
\Phi_{1,ij}^{kl} - \rho_{ij}^{kl} - T_{ij}^{kl} + I_{ij}^{kl} & & - \lambda_1 N_{1,ij}^{kl} &= 0 \\
\Phi_{2,ij}^{kl} - \rho_{ij}^{kl} - T_{ij}^{kl} + (f_1^2/f_2^2) I_{ij}^{kl} & - \lambda_2 N_{2,ij}^{kl} &= 0 \\
P_{1,ij}^{kl} - \rho_{ij}^{kl} - T_{ij}^{kl} - I_{ij}^{kl} & & &= 0 \\
P_{2,ij}^{kl} - \rho_{ij}^{kl} - T_{ij}^{kl} - (f_1^2/f_2^2) I_{ij}^{kl} & & &= 0
\end{aligned}
\qquad (9)
$$

The fundamental observation equations for pseudorange and carrier phase observations, parameterized according to the generalization-based approach, are presented in Eq. 9, where the notation follows the previously explained paradigm. Stochastic constraints are applied to the atmospheric corrections and the LAMBDA method is used for the AR. All the processing is carried out at the rover receiver in the instantaneous mode. The success of the instantaneous GPS positioning over long baselines depends on the ability to resolve the integer phase ambiguities. The performance of the method strongly depends on the quality of the atmospheric corrections provided from the network. If high quality corrections are available, the method becomes virtually distance-independent. The analyses presented in Section 3 are aimed at estimating the required quality of these corrections to assure seamless, instantaneous positioning without any initialization, as required in the on-the-fly (OTF) technique.

All the processing algorithms currently implemented in the MPGPS™ software include the following modules: long-range instantaneous and OTF RTK GPS, precise point positioning (PPP), multi-station DGPS, ionosphere
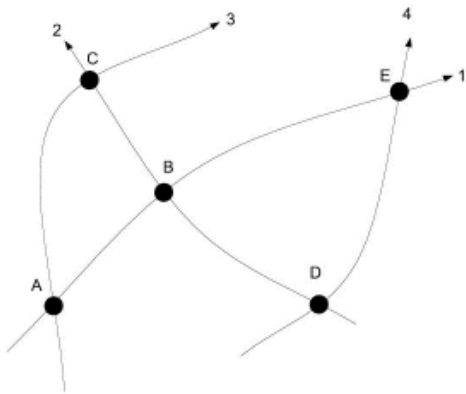
Fig. 1 A "triangle" ABC formed by 3 tracks and 3 crossovers; Adjoining "triangles" showing four tracks (unknowns) and five crossovers (observations), provide redundancy (Smith, 2004).
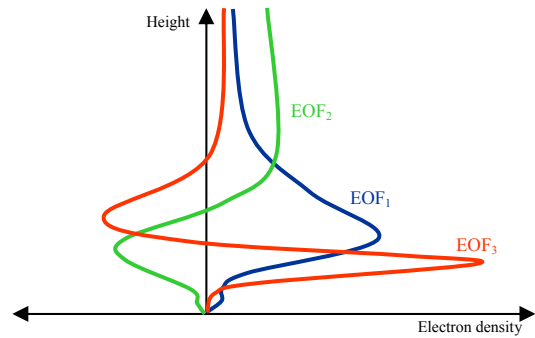

Fig. 2 Examples of empirical orthonormal functions (Spencer *et al.*, 2004).

Fig. 3a The CORS subnetwork used in the experiments.

Fig. 3b The baselines analyzed in the experiments.

modeling and mapping, and troposphere modeling. The software operates in static, kinematic and instantaneous modes, and can provide solutions in the network as well as in the baseline mode. More details on the instantaneous positioning algorithms can be found in (Kashani *et al.*, 2004a and 2004b; Wielgosz *et al.*, 2004; Grejner-Brzezinska *et al.*, 2004a and 2004b).

3 Test data and experimental results

3.1 Test data set and data processing strategy

A 24-hour GPS data set collected by the Ohio CORS stations on August 31, 2003, with a 30 s sampling rate, was used in the experiments described in the following sections. The 24-hour data set allowed for a comparison of the time windows with different ionospheric TEC

levels and varying GPS constellations. Figure 3 illustrates the selected reference subnetwork (3a) and the baselines processed and analyzed here (3b). Station KNTN was selected as an unknown rover, whose "true" coordinates were obtained and analyzed from a 24-hour static solution of the Ohio CORS network using the BERNESE software. The MPGPS™ software was used to first process the five-station network (KNTN, COLB, SIDN, DEFI, TIFF) to derive the tropospheric and ionospheric corrections that formed the reference "truth" (MPGPS-L4) in the test comparing the ionospheric models. Next, the four-station network, where the simulated "rover" was removed from the solution, was used to derive the atmospheric reference corrections (TZD and ZD ionospheric corrections - MPGPS-NR), which were then interpolated to the rover location, and applied in the baseline solutions presented in Section 3.3.

3.2 The ionospheric model analysis

The five ionospheric models (MPGPS-P4, MPGPS-NR, IGS GIM, ICON and MAGIC), as explained earlier, were

Tab. 1 DD ionospheric delay residual statistics (±5 cm and ±10 cm cut-off) for 24 h.

	Residuals in % within predefined limits, 24 h			
	KNTN-SIDN (~60 km)		KNTN-DEFI (~100 km)	
	±10 cm	±5 cm	±10 cm	±5 cm
MPGPS-P4	66.8	31.5	75.3	48.7
MPGPS-NR	99.3	94.2	99.3	94.2
IGS GIM	94.9	71.4	81.7	54.3
ICON	58.4	31.9	58.2	32.5
MAGIC	98.0	83.3	90.1	67.1

Tab. 2 DD ionospheric delay residual statistics ±5 cm and ±10 cm cut-off) for 2-hour session 04:00–06:00 UTC.

	Residuals in % within predefined limits, 04:00–06:00 UTC			
	KNTN-SIDN (~60 km)		KNTN-DEFI (~100 km)	
	±10 cm	±5 cm	±10 cm	±5 cm
MPGPS-P4	79.8	71.5	79.8	48.7
MPGPS-NR	97.0	84.1	97.0	84.1
IGS GIM	90.7	63.7	70.8	37.3
ICON	70.0	40.8	42.0	22.2
MAGIC	94.5	78.6	86.1	62.4

Tab. 3 DD ionospheric delay residual statistics (±5 and ±10 cm cut-off) for 2-hour session 18:00–20:00 UTC.

	Residuals in % within predefined limits, 18:00–20:00 UTC			
	KNTN-SIDN (~60 km)		KNTN-DEFI (~100 km)	
	±10 cm	±5 cm	±10 cm	±5 cm
MPGPS-P4	59.9	39.9	66.0	36.3
MPGPS-NR	100.0	100.0	100.0	100.0
IGS GIM	98.1	69.8	88.6	55.9
ICON	75.2	26.1	93.5	63.4
MAGIC	99.9	91.5	98.2	83.5

used to derive DD ionospheric corrections for two baselines formed by the rover and two different reference stations (baseline KNTN-SIDN is ~60 km long, and KNTN-DEFI is ~100 km long). Figures 4 and 6 illustrate the estimated corrections for both baselines, while Figures 5 and 7 display the residuals with respect to the reference "truth" (MPGPS-L4). The time scale is shown in UTC time, with the zero epoch corresponding to UTC midnight (five hours ahead of Eastern Standard Time, i.e., the local time).

As can be observed in Figures 4 and 6, the ionosphere variability changes during the course of the day, and seems to be slightly more variable during the local night, as compared to the local day. It is quite opposite to the standard ionospheric behavior; however, the ionospheric gradients were indeed higher during the night, indicating greater ionospheric activity. The maximum Kp index for that day was 2o.

It can be observed from Figures 5 and 7 that the MPGPS-P4 model displays a very smooth signature of differences from the reference "truth"; this is primarily due to the fact that both solutions are based essentially on actual carrier phase data (i.e., phase-smoothed pseudoranges). The

OSU network RTK model (MPGPS-NR) shows a good fit to the reference "truth," while the IGS GIM model displays bigger departures from the reference solution. This can be explained by the fact that GIM has lower spatial and temporal resolution, and thus it is subject to some smoothing effects. Still, the fit is approximately at the level of about 1.0 L1 cycle.

The NGS ICON model displays a rather flat spectrum of differences with respect to the reference "truth"; however, some biases are visible in the figures. The ionospheric signature of both the "truth" and the ICON models are very similar, as both were derived from carrier phase data. The ICON solution may be subject to incorrectly resolved biases, primarily due to the very strict procedure of cycle slip detection and fixing, and due to using a simple cosine mapping function at crossovers. This matter is currently under detailed investigation, and once it is resolved, this model is expected to provide high-quality ionospheric corrections for precise positioning.

The comparison of MAGIC to the reference "truth" indicates a fit similar to the signature shown for the IGS GIM. Again, this model is subject to smoothing due to

the time quantization of the final output, as already explained. Still, the fit is good, reaching a maximum of around 0.5–1.0 L1 cycle. It should be pointed out that the apparent discontinuities, which can be observed in the ionospheric model plots are in fact not real, and are due to the fact that the reference satellite was changed every two hours, so each 2-hour session displays an essentially different DD ionosphere.

In analyzing the differences between each model and the reference "truth" the following should be considered: the MPGPS-NR differences with respect to the "true" DD ionosphere are not base-rover distance-dependent, as the errors in the DD ionospheric correction come only from the undifferenced (and thus, biased) ionospheric correction interpolated for the rover location. The accuracy of the ionospheric estimate at the reference stations is considered uniformly biased per satellite; thus the bias is removed by forming the DD in the rover positioning procedure. In case of the MPGPS-P4 model the errors are also distance-independent since they arise from the undifferenced ambiguity estimation for a particular satellite-station pair during the carrier phase smoothing procedure. The biased ambiguities, and thus the ionospheric delay estimates, are station-dependent and completely random. The behavior of the ICON model is similar to that of MPGPS-P4. Namely, the undifferenced ambiguities are satellite-station-specific, and the amount of bias that affects them is random. To the contrary, both MAGIC and GIM models do not display station- or station-satellite dependence, but both are rather distance-dependent, and thus, the error in the ionospheric correction is bigger for longer baselines.

The summary statistics for the ionospheric model comparison is shown in Table 1, which covers the entire 24-hour session. Since the behavior of the ionosphere and the models changes over the course of the day (see Figures 4–7), two representative 2-hour windows (04:00–06:00 UTC, corresponding to roughly the local midnight; and 18:00–20:00 UTC, representing the local daytime window) were selected, and the statistics are summarized in Tables 2 and 3. The tables show the percentage of the model differences from the reference "truth" that falls within ±5 cm and ±10 cm predefined limits.

3.3 Instantaneous RTK Positioning Analysis with MPGPS-NR Model

In order to assess the quality of the ionospheric correction in more absolute terms, the final rover positioning test was performed. The two baselines, selected earlier, were used to derive the coordinates of KNTN (the rover) using the MPGPS-NR ionospheric corrections for the two representative 2-hour windows, as explained in the

previous section. These windows correspond to the worst (04:00–06:00 UTC) and the best (18:00–20:00 UTC) quality of the MPGPS-NR ionospheric corrections (see Tables 4 and 5). The instantaneous positioning module from the MPGPS^{TM} software was used (i.e., single-epoch solution without OTF initialization), and the accuracy of the positioning results is illustrated in Figures 8–11. In order to emphasize the importance of the correct measure of the quality of the applied ionospheric corrections, several experiments were performed with the DD ionospheric corrections treated as fixed (0 sigma, which means the ionosphere is removed from the functional model) and as stochastic constraints, with the sigma varying from 1 cm to 5 cm. Examples of these analyses are shown next.

Figure 8 displays the n, e and u residuals of the rover coordinates with respect to the known station coordinates for the ~60 km baseline, where the initial standard deviation of the ionospheric corrections of 0 cm was used in the rover positioning algorithm. Clearly, the assumption that the external ionosphere is errorless was not correct for the "worst" window (04:00–06:00 UTC), while the "best" window (18:00–20:00 UTC) provides an excellent solution (with 100% of instantaneous AR success rate) under this assumption. The best solution for the "worst" window was obtained when the ionospheric correction was constrained to 5 cm, while this constraint was too loose for the "best" window, as shown in Figure 9. However, the instantaneous AR success rate for the "worst" window was only around 75 %. In case of the 100 km baseline, the sigma of 0 cm provided unsatisfactory results for both windows analyzed (see Figure 10), while a sigma of 1 cm for the ionospheric constraint was the best choice for the "best" window (with 100% of instantaneous AR success rate), and a sigma of 5 cm delivered the best positioning results (with around 70% of instantaneous AR success rate) for the "worst" window, as shown in Figure 11.

The positioning results discussed in this section were all derived using the MPGPS-NR ionospheric corrections that, based on the statistics provided in Tables 4 and 5, display the best fit to the reference "truth." The time windows analyzed in Tables 4 and 5 correspond to the 2-hour sessions illustrated in Figures 8–11. Clearly, the MPGPS-NR solution provides DD ionospheric corrections that fit the reference "truth" the best, and are usually sufficient to provide instantaneous centimeter-level positioning of the user. The other models discussed here offer lower rate of success in supporting instantaneous AR, and therefore the suitability of these models to support fast OTF AR is currently under investigation and will be reported in the next publication.
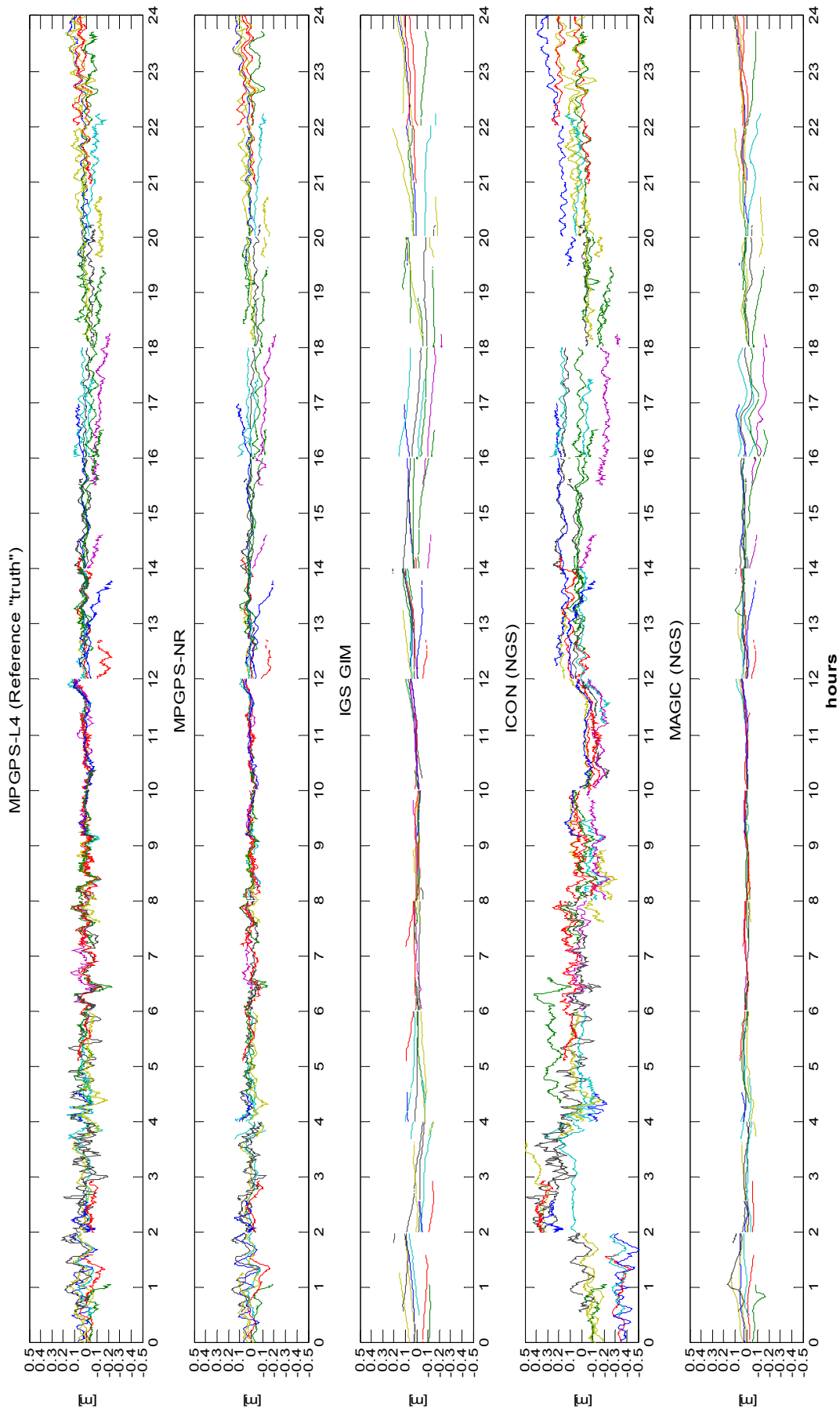
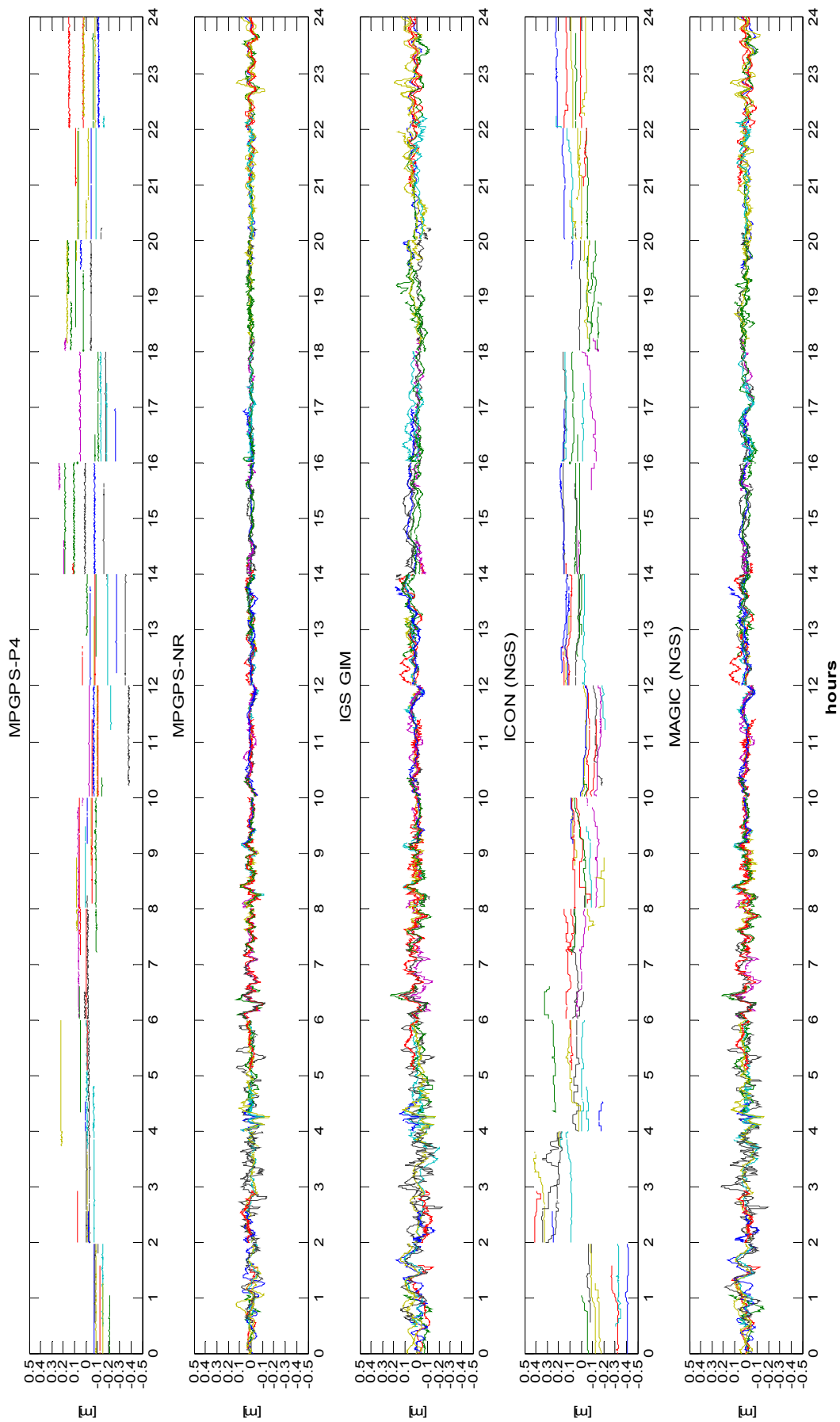Fig. 4 Estimated DD ionospheric corrections for the analyzed models — 24 h, KNTN-SIDN (~60 km).

Fig. 5 DD ionospheric residuals with respect to the reference "truth" — 24 h, KNTN-SIDN (~60 km).
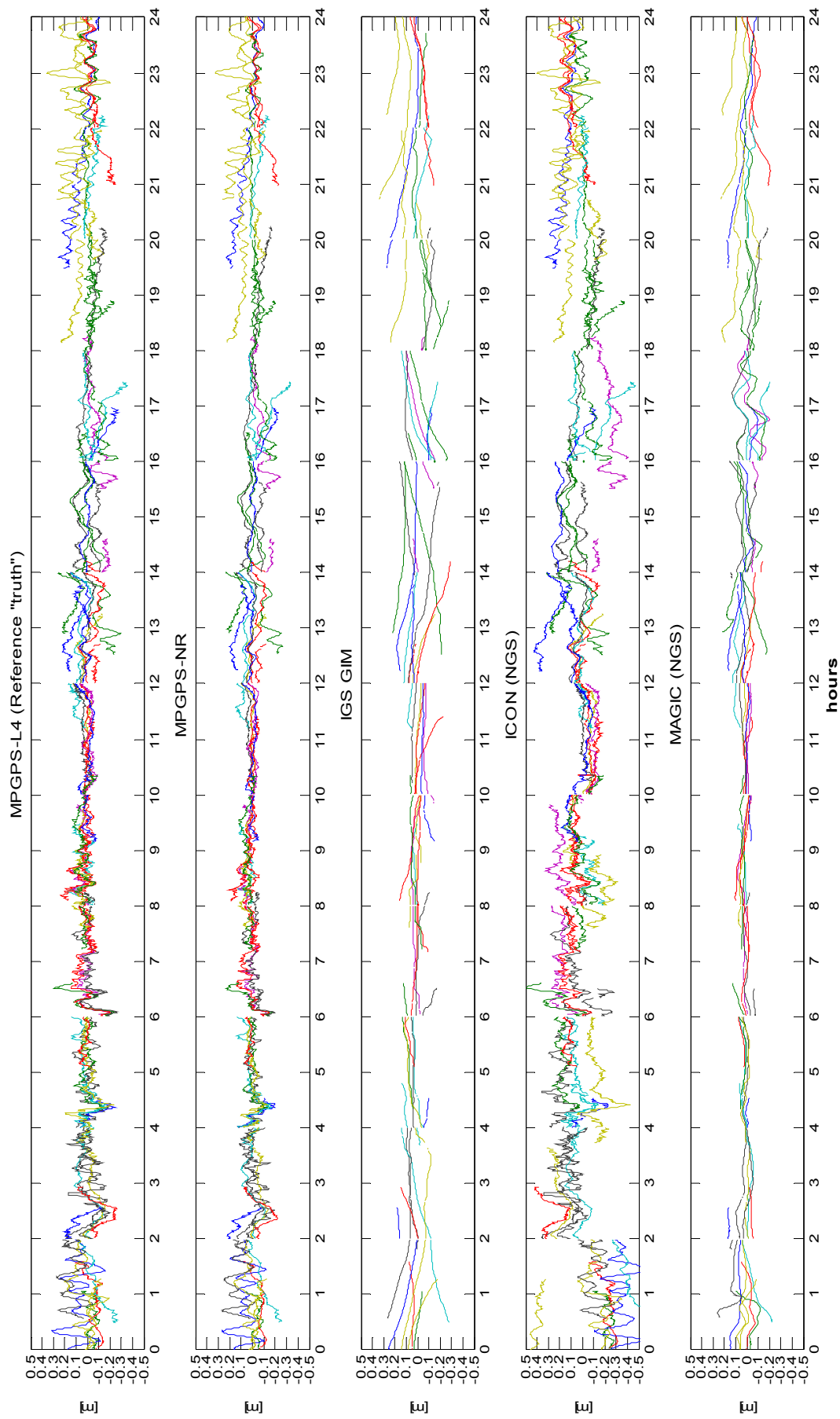
Fig. 6 Estimated DD ionospheric corrections for the analyzed models — 24 h, KNTN-DEFI (~100 km).

Journal of Global Positioning Systems
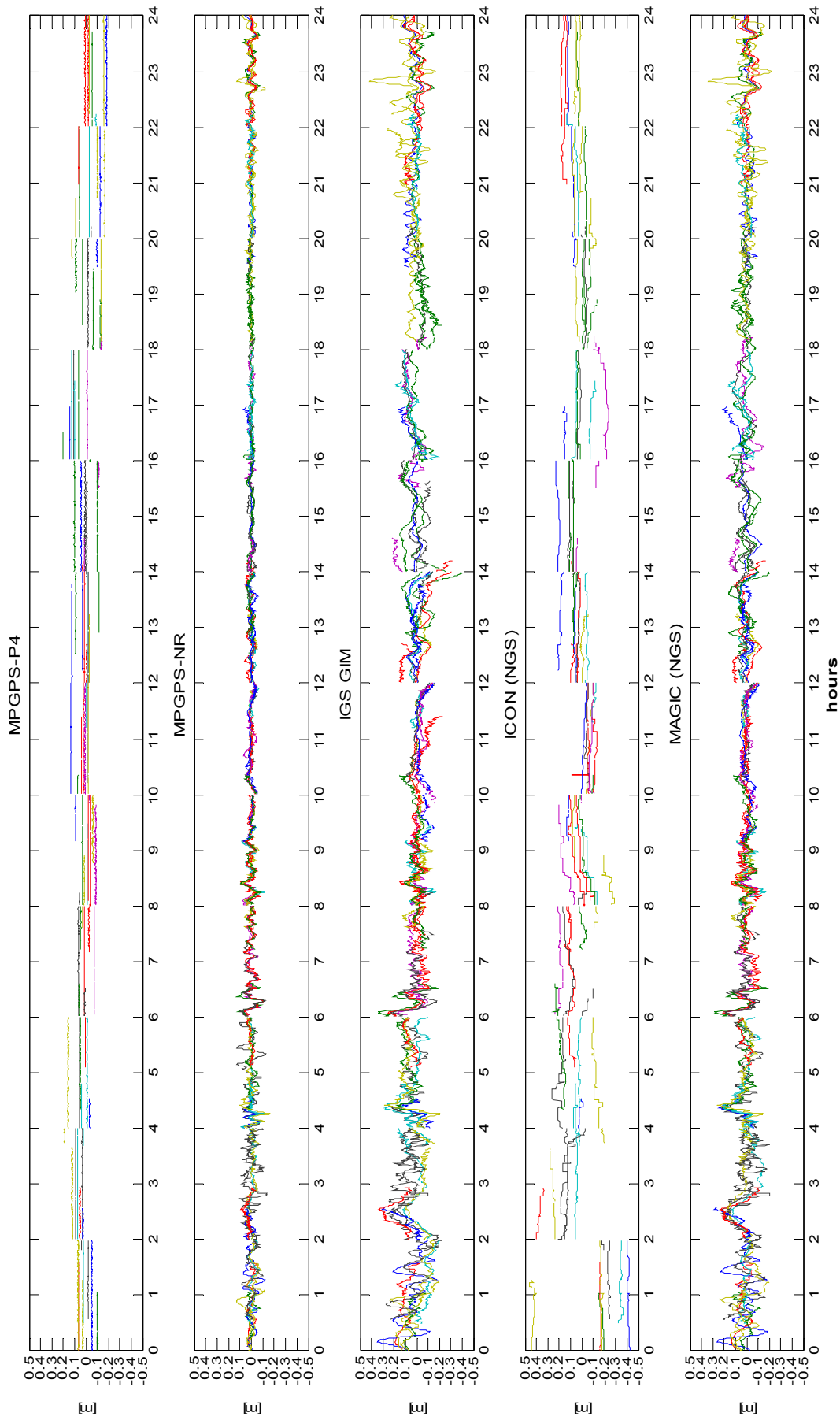
Fig. 7 DD ionospheric residuals with respect to the reference "truth" — 24 h, KNTN-DEFI (~100 km)

04:00 - 06:00 UTC

18:00 - 20:00 UTC

Fig. 8 Instantaneous RTK position residuals with respect to the known coordinates;
2-hour windows, KNTN-SIDN (~60 km); 0 cm constraint (1 sigma) was applied
to the ionospheric corrections.

04:00 - 06:00 UTC

18:00 - 20:00 UTC

Fig. 9 Instantaneous RTK position residuals with respect to the known coordinates;
2-hour windows, KNTN-SIDN (~60 km); 5 cm constraint (1 sigma) was applied
to the ionospheric corrections.

04:00 - 06:00 UTC

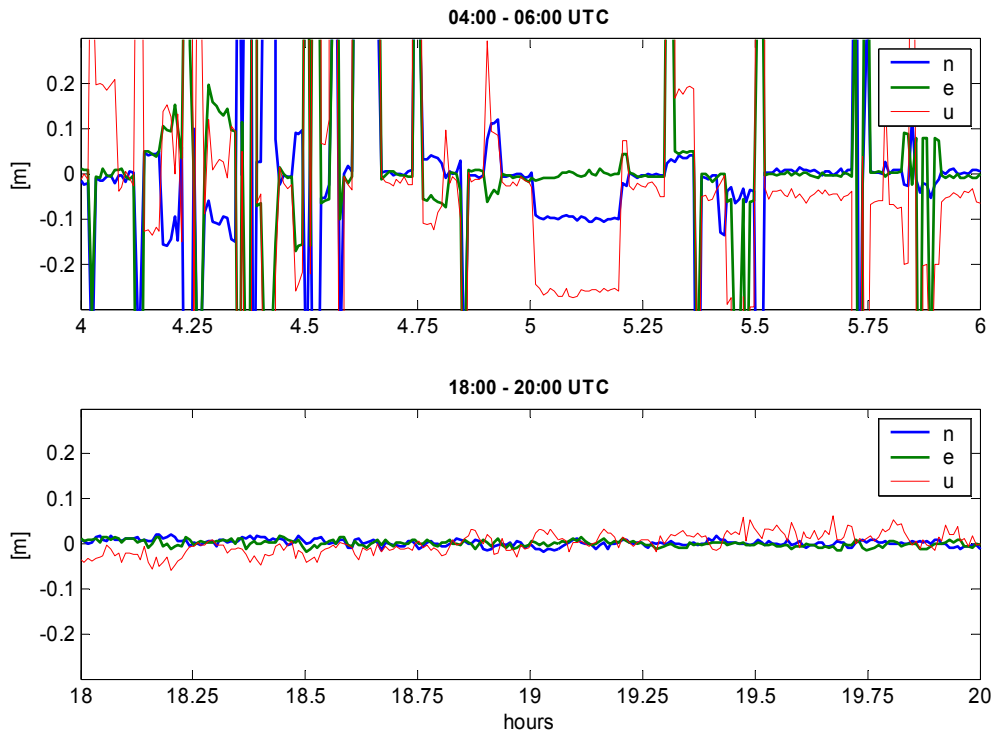**18:00 - 20:00 UTC**

Fig. 10 Instantaneous RTK position residuals with respect to the known coordinates;
2-hour windows, KNTN-DEFI (~100 km); 0 cm constraint (1 sigma) was applied
to the ionospheric corrections.
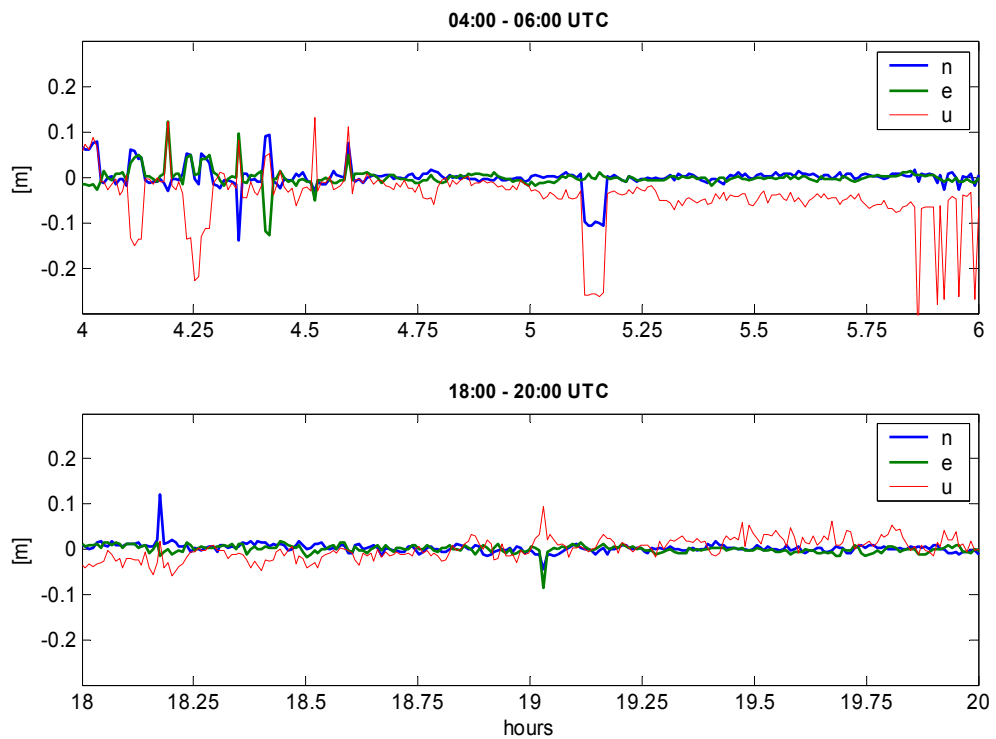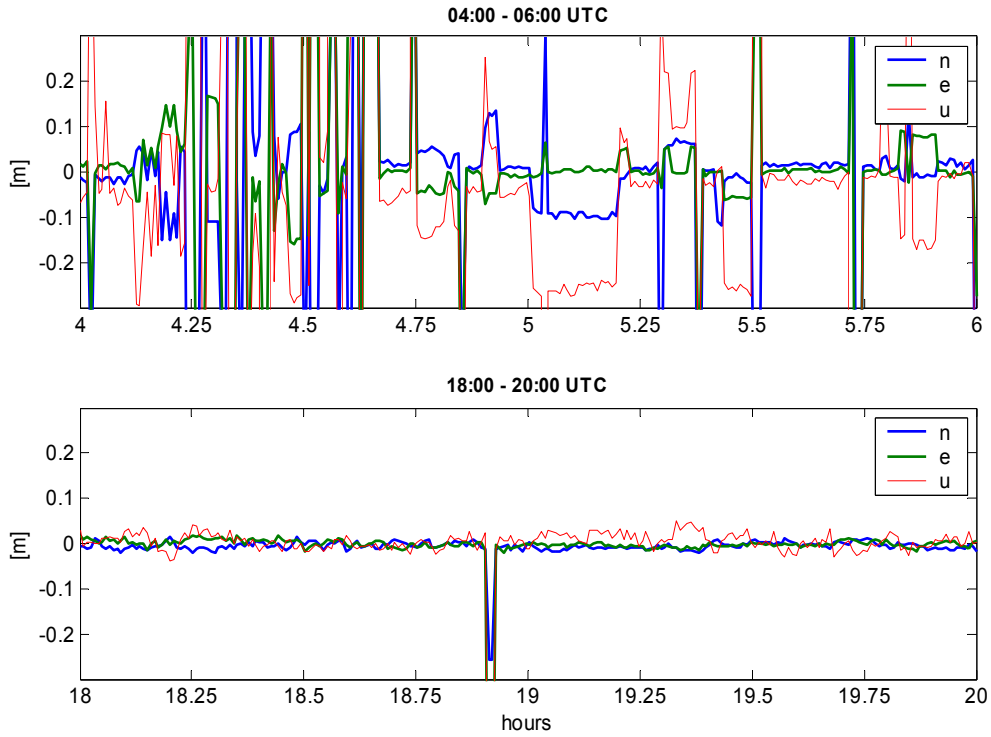
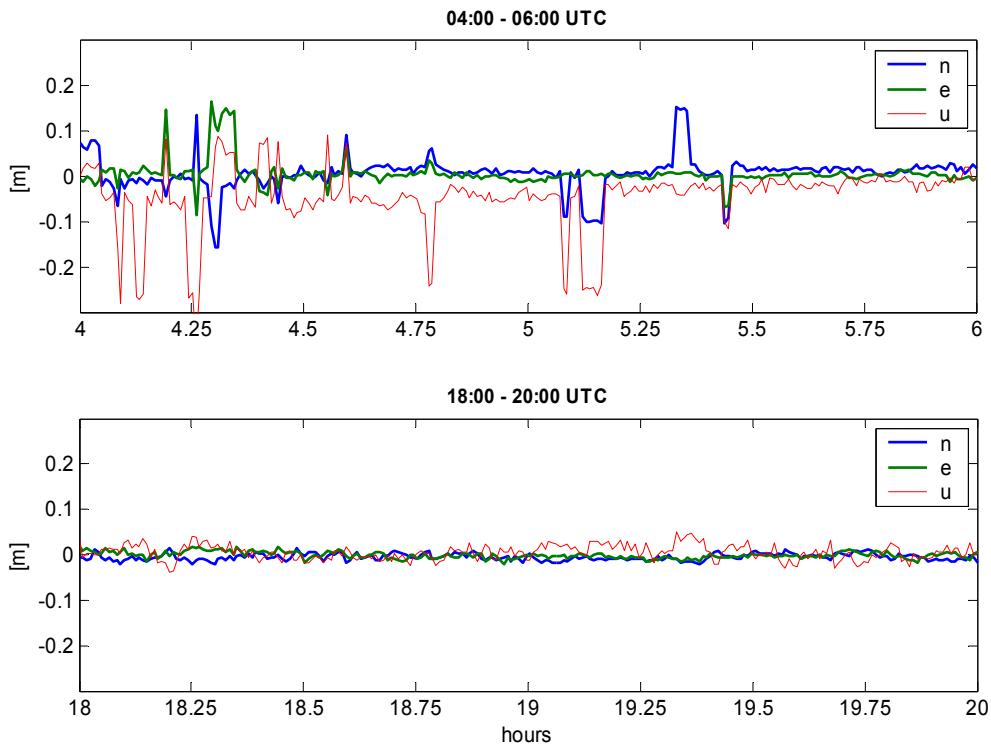**04:00 - 06:00 UTC**

18:00 - 20:00 UTC

Fig. 11 Instantaneous RTK position residuals with respect to the known coordinates;
2-hour windows, KNTN-DEFI (~100 km); 1 cm constraint (1 sigma) for the ionospheric correction
was applied to the "best" window (bottom) and 5 cm for the "worst" window (top).

Tab. 4 Mean and standard deviation (std) of DD ionospheric residuals with respect to the reference "truth"
for two 2-hour windows and ~60 km baseline (KNTN-SIDN).

KNTN-SIDN (~60 km)											
04:00–06:00 UTC						18:00–20:00 UTC					
mean [m]						mean [m]					
PRNs	MPGPS P4	MPGPS NR	IGS GIM	ICON	MAGIC	MPGPS P4	MPGPS NR	IGS GIM	ICON	MAGIC	PRNs
28 - 4	-0.01	-0.00	0.02	-0.01	-0.01	0.04	0.00	0.06	0.07	-0.01	25 - 1
28 - 7	-0.03	0.01	-0.02	0.04	-0.01	0.16	0.01	0.07	-0.11	-0.01	25 - 2
28 - 8	0.01	0.01	0.06	-0.17	-0.00	0.18	-0.01	-0.03	-0.13	0.03	25 - 5
28 - 9	0.05	-0.00	-0.05	0.24	0.00	0.08	0.01	-0.00	-0.03	-0.01	25 - 6
28 - 11	-0.07	-0.00	-0.05	-0.06	-0.02	-0.04	0.01	-0.03	0.01	0.03	25 - 14
28 - 20	0.22	0.00	-0.03	0.08	0.01	0.09	0.01	0.04	-0.06	-0.00	25 - 16
28 - 24	-0.01	0.01	0.05	0.09	0.02	0.16	0.01	0.03	-0.06	0.01	25 - 20
						0.13	-0.00	-0.02	-0.15	0.02	25 - 23
						0.02	0.01	-0.04	-0.10	0.01	25 - 30
std [m]						std [m]					
28 - 4	0.00	0.02	0.03	0.01	0.03	0.00	0.01	0.02	0.00	0.02	25 - 1
28 - 7	0.00	0.06	0.07	0.02	0.07	0.00	0.02	0.03	0.02	0.03	25 - 2
28 - 8	0.00	0.04	0.05	0.01	0.04	0.00	0.01	0.01	0.01	0.01	25 - 5
28 - 9	0.00	0.03	0.04	0.01	0.04	0.00	0.02	0.02	0.00	0.02	25 - 6
28 - 11	0.00	0.04	0.04	0.01	0.03	0.00	0.01	0.02	0.01	0.03	25 - 14
28 - 20	0.00	0.04	0.05	0.04	0.04	0.00	0.01	0.02	0.01	0.02	25 - 16
28 - 24	0.00	0.02	0.03	0.01	0.03	0.00	0.01	0.03	0.01	0.03	25 - 20
28 - 4	0.00	0.02	0.03	0.01	0.03	0.00	0.02	0.03	0.01	0.02	25 - 23
						0.00	0.01	0.03	0.02	0.02	25 - 30
						0.00	0.01	0.02	0.00	0.02	25 - 1

Tab. 5 Mean and standard deviation (std) of DD ionospheric residuals with respect to the reference "truth"
for two 2-hour windows and ~100 km baseline (KNTN-DEFI).

KNTN-DEFI (~100 km)											
04:00–06:00 UTC						18:00–20:00 UTC					
mean [m]						mean [m]					
PRNs	MPGPS P4	MPGPS NR	IGS GIM	ICON	MAGIC	MPGPS P4	MPGPS NR	IGS GIM	ICON	MAGIC	PRNs
28 - 4	-0.01	0.00	0.00	0.03	0.01	-0.10	0.01	0.08	0.06	-0.01	25 - 1
28 - 7	0.06	0.01	0.05	0.19	0.02	0.09	0.01	-0.02	-0.07	0.02	25 - 2
28 - 8	-0.03	0.01	-0.01	0.01	0.07	-0.14	-0.01	-0.02	-0.12	0.01	25 - 5
28 - 9	0.05	0.00	0.08	0.17	0.03	0.12	0.01	-0.01	-0.09	-0.01	25 - 6
28 - 11	0.04	0.00	0.13	0.07	0.06	-0.02	0.01	-0.04	-0.03	0.00	25 - 14

28 - 20	0.16	0.00	0.07	-0.12	0.01	0.03	0.01	-0.06	-0.01	-0.00	25 - 16
28 - 24	0.00	0.01	0.05	0.10	0.02	-0.13	0.01	0.04	0.04	0.02	25 - 20
						-0.13	-0.00	-0.13	-0.08	0.01	25 - 23
						-0.06	0.01	-0.04	-0.02	0.04	25 - 30
std [m]						**std [m]**					
28 - 4	0.00	0.02	0.05	0.01	0.06	0.00	0.01	0.02	0.01	0.03	25 - 1
28 - 7	0.00	0.06	0.07	0.03	0.07	0.00	0.02	0.04	0.01	0.04	25 - 2
28 - 8	0.00	0.04	0.09	0.01	0.10	0.00	0.01	0.03	0.01	0.03	25 - 5
28 - 9	0.00	0.03	0.05	0.02	0.05	0.00	0.02	0.03	0.02	0.04	25 - 6
28 - 11	0.00	0.04	0.07	0.01	0.08	0.00	0.01	0.02	0.01	0.02	25 - 14
28 - 20	0.00	0.04	0.08	0.03	0.06	0.00	0.01	0.04	0.01	0.03	25 - 16
28 - 24	0.00	0.02	0.05	0.02	0.04	0.00	0.01	0.02	0.01	0.03	25 - 20
28 - 4	0.00	0.02	0.05	0.01	0.06	0.00	0.02	0.04	0.03	0.05	25 - 23
						0.00	0.01	0.03	0.01	0.04	25 - 30
						0.00	0.01	0.02	0.01	0.03	25 - 1

4 Summary and conclusions

The analysis of the quality of the network-based ionospheric correction derived from five independent models was presented, and the applicability of these models to support instantaneous AR and kinematic positioning were tested and discussed. The CORS and/or IGS reference network GPS data were used to derive the model corrections. One of the CORS stations in Ohio was selected as an unknown rover location, and its coordinates were estimated in the simulated kinematic mode using the OSU-developed MPGPS™ software. The successful instantaneous AR was achieved with the MPGPS-NR model, whose quality (1 sigma) is estimated as 1–6 cm, as shown in Tables 4 and 5. Clearly, this accuracy, corresponding to around one quarter of the L1 cycle, can generally assure an accurate instantaneous AR for longer baselines; however, the level of success is a function of the level of ionospheric variability. The remaining models are currently tested for their applicability to OTF AR in terms of the speed of AR, i.e., the number of epochs needed to find integers and the resulting quality of the position coordinates. These findings will be reported in a subsequent publication.

Acknowledgement:

References

Bilitza D. (1997): *International Reference Ionosphere — Status 1995/96*. Advances in Space Research, Vol. 20, No. 9, 1751–1754.

Feltens J.; N. Jakowski (2002): *The International GPS Service (IGS) Ionosphere Working Activity*. SCAR Report No. 21.

Bock Y.; de Jonge P.; Honcik, D.; Fayman, J. (2003): *Wireless Instantaneous Network RTK: Positioning and Navigation*, Proceedings of ION GPS/GNSS, September 9–12, Portland, OR, pp. 1397–1405.

Grejner-Brzezinska D.A.; Kashani I.; Wielgosz P. (2004a): *Analysis of the Network Geometry and Station Separation for Network-Based RTK.* Proceedings of ION NTM, January 26–28, San Diego, CA, 469–474.

Grejner-Brzezinska D. A.; Kashani I.; Wielgosz P. (2004b): *On Accuracy and Reliability of Instantaneous Network RTK as a Function of Network Geometry, Station Separation, and Data Processing Strategy*. Submitted to GPS Solutions, September 2004.

Hugentobler U.; Schaer S.; Fridez P. (2001): *BERNESE GPS Software Version 4.2*. Astronomical Institute, University of Berne, Switzerland.

Kim, D.; Langley, R.B. (2000): *GPS Ambiguity Resolution and Validation: Methodologies, Trends and Issues*. Proceedings of 7th GNSS Workshop and International Symposium on GPS/GNSS, Seoul, Korea, November 30 – December 2, 213–221.

Kashani I.; Grejner-Brzezinska D.A.; Wielgosz P. (2004a): *Towards instantaneous RTK GPS over 100 km distances*. Proceedings of ION 60th Annual Meeting, June 7–9, 2004, Dayton, Ohio, 679–686.

Kashani I.; Wielgosz P.; Grejner-Brzezinska D.A. (2004b): ***The Effect of Double-Difference Ionospheric Corrections Latency on Instantaneous Ambiguity Resolution in Long-Range RTK***. ION GNSS 2004, September 21–24, Long Beach, California, 2881–2890.

Odijk D. (2000): ***Weighting Ionospheric Corrections to Improve Fast GPS Positioning Over Medium Distances***. Proceedings of ION GPS, September 19–22, Salt Lake City, UT, 1113–1123.

Odijk D. (2001): ***Instantaneous GPS Positioning Under Geomagnetic Storm Conditions***. GPS Solutions, Vol. 5, No. 2, 29–42.

Rizos C. (2002): ***Network RTK research and implementation: A geodetic perspective***. Journal of Global Positioning Systems, Vol. 1, No. 2, 144–150.

Schaer S. (1999): ***Mapping and Predicting the Earth's Ionosphere Using the Global Positioning System***. Ph.D. Thesis, Astronomical Institute, University of Berne.

Schaer S.; Gurtner W.; Feltens J. (1998): ***IONEX The IONosphere Map EXchange Format Version 1***. Proceedings of the IGS Analysis Center Workshop, ESA/ESOC, February 9–11, Darmstadt, Germany, 233–247.

Smith D.A. (2004): ***Computing unambiguous TEC and ionospheric delays using only carrier phase data from NOAA's CORS network***. Proceedings of IEEE PLANS 2004, April 26-29, Monterey, California, 527-537.

Spencer P.S.J.; Robertson D.S.; Mader, G.L. (2004): ***Ionospheric data assimilation methods for geodetic applications***. Proceedings of IEEE PLANS 2004, Monterey, California, April 26-29, 2004, 510-517.

Springer T.A. (1999): ***Modeling and Validating Orbits and Clocks Using the Global Positioning System***. Ph.D. dissertation, Astronomical Institute, University of Berne, Switzerland.

Teunissen P.J.G. (1994): ***A new method for fast carrier phase ambiguity estimation***. Proceedings of IEEE PLANS'94, Las Vegas, NV, April 11–15, 562–573.

Teunissen P.J.G.; Joosten P.; Tiberius C. (2002): ***A Comparison of TCAR, CIR and LAMBDA GNSS Ambiguity Resolution***. Proceedings of the ION GPS 2002, 24–27 September 2002, Portland, OR, 2799–2808.

Vollath U.; Buecherl A.; Landau H.; Pagels C.; Wagner B. (2000): ***Multi-Base RTK Positioning Using Virtual Reference Stations***. Proceedings of ION GPS, 19–22 September 2000, Salt Lake City, UT, 123–131.

Wanninger L. (2002): ***Virtual Reference Stations for Centimeter-Level Kinematic Positioning***. Proceedings of ION GPS 2002, September 24–27, Portland, Oregon, 1400–1407.

Wielgosz P.; Grejner-Brzezinska D.A.; Kashani I.; (2003): ***Regional Ionosphere Mapping with Kriging and Multiquadric Method***s. Journal of Global Positioning Systems, Vol. 2, Issue 1, 48–55.

Wielgosz P.; Grejner-Brzezinska D.; Kashani I. (2004): ***Network Approach to Precise GPS Navigation***. Navigation, Vol. 51, No. 3, 213–220.